AJNR

Low-cost high-resolution fast spin-echo MR of acoustic schwannoma: an alternative to enhanced conventional spin-echo MR?

R W Allen, H R Harnsberger, C Shelton, B King, D A Bell, R Miller, J L Parkin, R I Apfelbaum and D Parker

AJNR Am J Neuroradiol 1996, 17 (7) 1205-1210
http://www.ajnr.org/content/17/7/1205

Low-Cost High-Resolution Fast Spin-Echo MR of Acoustic Schwannoma: An Alternative to Enhanced Conventional Spin-Echo MR?

Robert W. Allen, H. Ric Harnsberger, Clough Shelton, Brian King, Don Antonio Bell, Ronald Miller, James L. Parkin, Ron I. Apfelbaum, and Dennis Parker

PURPOSE: To determine whether unenhanced high-resolution T2-weighted fast spin-echo MR imaging provides an acceptable and less expensive alternative to contrast-enhanced conventional T1-weighted spin-echo MR techniques in the diagnosis of acoustic schwannoma. **METHODS:** We reviewed in a blinded fashion the records of 25 patients with pathologically documented acoustic schwannoma and of 25 control subjects, all of whom had undergone both enhanced conventional spin-echo MR imaging and unenhanced fast spin-echo MR imaging of the cerebellopontine angle/internal auditory canal region. The patients were imaged with the use of a quadrature head receiver coil for the conventional spin-echo sequences and dual 3-inch phased-array receiver coils for the fast spin-echo sequences. **RESULTS:** The size of the acoustic schwannomas ranged from 2 to 40 mm in maximum dimension. The mean maximum diameter was 12 mm, and 12 neoplasms were less than 10 mm in diameter. Acoustic schwannoma was correctly diagnosed on 98% of the fast spin-echo images and on 100% of the enhanced conventional spin-echo images. Statistical analysis of the data using the κ coefficient demonstrated agreement beyond chance between these two imaging techniques for the diagnosis of acoustic schwannoma. **CONCLUSIONS:** There is no statistically significant difference in the sensitivity and specificity of unenhanced high-resolution fast spin-echo imaging and enhanced T1-weighted conventional spin-echo imaging in the detection of acoustic schwannoma. We believe that the unenhanced high-resolution fast spin-echo technique provides a cost-effective method for the diagnosis of acoustic schwannoma.

Index terms: Magnetic resonance, comparative studies; Neuroma; Temporal bone, magnetic resonance

AJNR Am J Neuroradiol 17:1205–1210, August 1996

Acoustic schwannoma is the most common mass of the cerebellopontine angle found to be responsible for unilateral sensorineural hearing loss (1–3). The current imaging test of choice for the diagnosis of acoustic schwannoma is contrast-enhanced conventional spin-echo magnetic resonance (MR) imaging (4, 5). This technique has high sensitivity and specificity for the diagnosis of this entity, but requires the use of an intravenously administered contrast agent.

Submillimeter-resolution MR imaging of the inner ear and internal auditory canal has been investigated using gradient-echo techniques (6, 7). However, the theoretical advantages of thin-section gradient-echo imaging are more than outweighed by the magnetic susceptibility–related signal loss seen in the temporal bone as a result of diverse tissue interfaces inherent to this area. Fast spin-echo imaging has been shown to be significantly less affected by these artifacts, allowing the acquisition of high-resolution T2-weighted images of the inner ear, internal auditory canal, and cerebellopontine angle (8).

The central goal of this study was to assess the value of unenhanced high-resolution T2-

Received November 2, 1995; accepted after revision February 14, 1996.

From the Departments of Radiology (R.W.A., H.R.H., B.K., D.A.B., R.M., D.P.), Otolaryngology, Head & Neck Surgery (C.S., J.L.P.), and Neurosurgery (R.I.A.), University of Utah Health Sciences Center, Salt Lake City.

Address reprint requests to H. Ric Harnsberger, MD, Department of Radiology, University of Utah Health Sciences Center, 50 N Medical Dr, Salt Lake City, UT 84132.

AJNR 17:1205–1210, Aug 1996 0195-6108/96/1707–1205

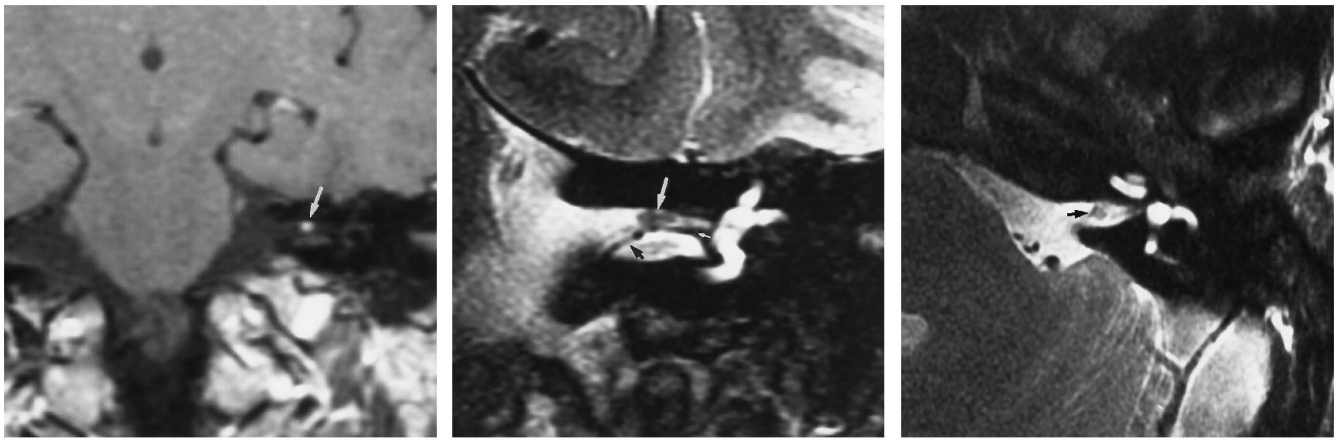

Fig 1. An intracanalicular acoustic schwannoma, 1 × 2 × 2 mm in diameter.

A, Enhanced coronal T1-weighted conventional spin-echo MR image shows the small acoustic schwannoma (*arrow*) in the left internal auditory canal.

B, Coronal high-resolution fast spin-echo MR image of the left internal auditory canal/cerebellopontine angle shows the small acoustic schwannoma as a filling defect seen within the high-signal cerebrospinal fluid (*large white arrow*). *Black arrow* indicates anterior inferior cerebellar artery loop in the internal auditory canal; *small white arrow*, crista falciformis.

C, Axial high-resolution fast spin-echo MR image again shows the intracanalicular acoustic schwannoma (*arrow*).

weighted fast spin-echo imaging with dual 3-inch phased-array temporomandibular joint receiver coils in the evaluation of acoustic schwannoma. We conducted a blinded review and comparison of unenhanced fast spin-echo images with enhanced T1-weighted conventional spin-echo images to answer the following question: Can acoustic schwannoma be reliably diagnosed without contrast enhancement using fast spin-echo techniques?

Materials and Methods

Twenty-five patients with pathologically documented acoustic schwannoma and 25 age-matched control subjects with no subjective disorders were examined on a 1.5-T MR unit (Signa, GE Medical Systems, Milwaukee, Wis, 5.X level software). The age range of the patients was 20 to 83 years (average, 49 years), and the size of the neoplasms ranged from 2 to 40 mm in maximum dimension. Twelve of the neoplasms were less than 10 mm in maximum diameter.

The T2-weighted fast spin-echo technique involved imaging patients with dual 3-inch phased-array receiver multicoils fixed in a temporomandibular joint holder with the coils centered over the external meatus. The following fast spin-echo sequence was performed in the axial and coronal planes: 5000/102/4 (repetition time [TR]/effective echo time/excitations); echo train length of 16; 512 × 384 matrix; 17-cm field of view; fat saturation; anterior, posterior, superior, and inferior saturation bands; and 3-mm contiguous sections. Scan time was 8 minutes. Flow compensation and physiologic gating were not used. The patients were then placed in a quadrature head coil and imaged with the use of a standard conventional spin-echo acoustic schwannoma protocol that included noncontrast coronal T1-weighted images of the internal auditory canal/cerebellopontine angle, axial whole-brain T2-weighted images, and contrast-enhanced axial and coronal T1-weighted images of the internal auditory canal/cerebellopontine angle.

Four neuroradiologists who were blinded to the clinical findings retrospectively reviewed the unenhanced T2-weighted fast spin-echo and enhanced T1-weighted conventional spin-echo images of all patients. The review was done in an independent, randomized fashion with the fast spin-echo and enhanced T1-weighted conventional spin-echo images read separately. The neuroradiologists were asked to assess the internal auditory canal/cerebellopontine angle region on each image for the presence of an acoustic schwannoma; each image was judged as positive or negative for acoustic schwannoma, with a confidence level assigned from 1 (definitely not present) to 5 (definitely present). If a neoplasm was present, its size and location were noted.

Results

The size of the neoplasms ranged from 1 × 1 × 2 mm (Fig 1) to 30 × 35 × 40 mm. The average tumor size was 9 × 9 × 12 mm, with 12 neoplasms measuring less than 10 mm in maximum diameter (Fig 2). All measurements were obtained from enhanced conventional spin-echo images.

A total of 400 observer evaluations were

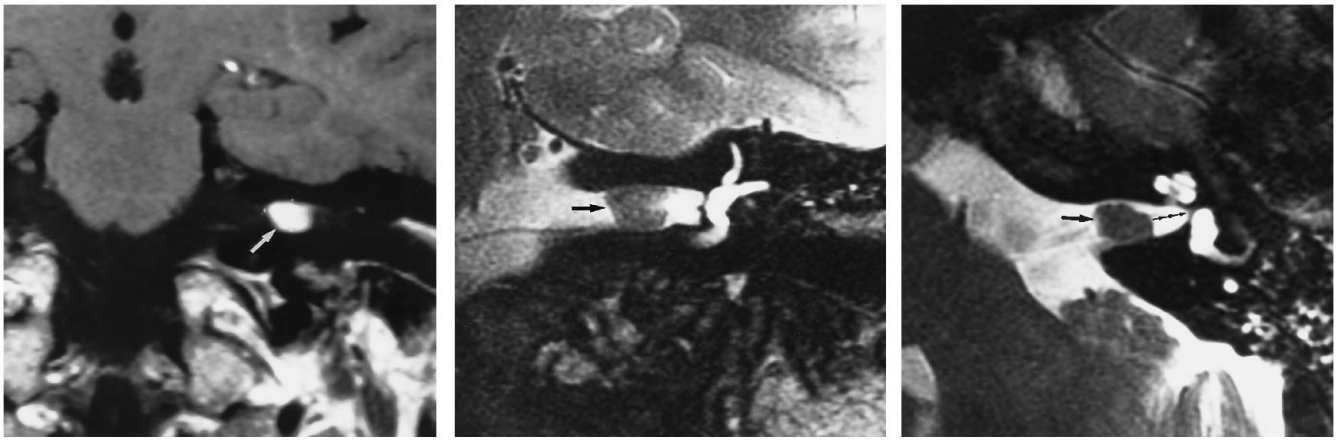

Fig 2. An intracanalicular acoustic schwannoma, 4 × 5 × 5 mm in diameter.

A, Enhanced coronal T1-weighted conventional spin-echo MR image reveals the acoustic schwannoma in the left internal auditory canal (*arrow*).

B, Coronal high-resolution fast spin-echo MR image focused on the left internal auditory canal/cerebellopontine angle shows the acoustic schwannoma as a large filling defect within the high-signal cerebrospinal fluid (*arrow*). The exact distance to the fundus can be measured for surgical planning as desired.

C, Axial fast spin-echo MR image of the left ear again shows the intracanalicular acoustic neuroma (*large arrow*). Notice how easily the distance to the fundus (*small arrows*) can be assessed on the fast spin-echo high-resolution images.

made. Internal auditory canal/cerebellopontine angle evaluations graded as 1 to 3 were considered to be negative responses and those graded as 4 or 5 were considered to be positive responses for acoustic schwannoma. Applying these criteria, acoustic schwannoma was correctly diagnosed on 98% (98 of 100) of the unenhanced high-resolution fast spin-echo images (four observers analyzing 25 positive internal auditory canal/cerebellopontine angle areas) and on 100% (100 of 100) of the enhanced conventional spin-echo images. Two false-negative results were obtained, both of which involved small neoplasms (4 mm or less) located in small internal auditory canals on fast spin-echo sequences.

Counting the opposite asymptomatic internal auditory canal/cerebellopontine angle regions of the 25 patients with acoustic schwannoma and the 50 normal regions of the 25 control subjects, a total of 75 normal internal auditory canal/cerebellopontine angle regions were evaluated by the four observers. Among the contrast-enhanced T1-weighted conventional spin-echo images, one false-positive finding was made out of the total of 300 observations (75 normal internal auditory canal/cerebellopontine angles × four observers = 300 total observations). A small fatty marrow space adjacent to the internal auditory canal was misdiagnosed one time as a small acoustic schwannoma. One false-positive finding was also made in the group of 300 T2-weighted observations. In this case, the internal auditory canal was small and the bunching of the nerve bundles was misdiagnosed as a small acoustic schwannoma. For both groups, then, the normal internal auditory canal/cerebellopontine angle was diagnosed correctly 99.7% (299 of 300) of the time.

The κ coefficient, a measure of agreement, was calculated for each observer in order to assess agreement beyond chance between these two diagnostic tests. The calculated κ values represented agreement between the enhanced conventional spin-echo images and the unenhanced fast spin-echo images for the diagnosis of acoustic schwannoma (9). The κ statistics and P values for the four observers were as follows: reviewer 1, $\kappa = 1.000$, $P < .0001$; reviewer 2, $\kappa = 0.956$, $P < .0001$; reviewer 3, $\kappa = 1.000$, $P < .0001$; and reviewer 4, $\kappa = 0.913$, $P < .0001$. The low P values, all less than .0001, confirm the statistical significance of the calculated κ coefficients.

Discussion

Unilateral sensorineural hearing loss in the adult sends the referring physician looking for acoustic schwannoma as a treatable cause of this symptom. However, because whole-brain and focused internal auditory canal/cerebel-

lopontine angle unenhanced and enhanced conventional spin-echo MR studies are expensive, the clinician often puts the patient through multiple tests (audiometric testing, impedance testing, brain stem evoked response) to decide whether MR imaging in search of acoustic schwannoma is necessary. Despite this battery of tests, the yield of complete MR studies designed to look for this tumor is quite low. If an accurate, rapid, low-cost limited MR examination aimed at the diagnosis of acoustic schwannoma could be devised, it might be possible to avoid these multiple initial tests, moving the patient directly from the abnormal audiogram to this limited MR study.

The first step toward such a limited MR examination is to develop an idealized pulse sequence aimed at the diagnosis of mass lesions, especially acoustic schwannoma, of the internal auditory canal/cerebellopontine angle area. A comparison of this technique with the present standard comes next. Enhanced conventional spin-echo T1-weighted MR imaging is currently the standard of reference for evaluating disease of the internal auditory canal/cerebellopontine angle (4, 5). High-resolution imaging methods such as three-dimensional gradient-recalled acquisition in the steady state (GRASS), enhanced 3-D fast imaging with steady-state precession (FISP), and unenhanced fast spin-echo sequences have been proposed as alternatives (6, 7, 10). Magnetic susceptibility artifacts, inherent to the 3-D GRASS and 3-D FISP sequences, limit spatial resolution and decrease the signal-to-noise ratio. These artifacts are especially prominent in the region of the internal auditory canal, where small soft-tissue structures interface with surrounding bone and air (8, 11). In contradistinction, fast spin-echo sequences, with their multiple closely spaced 180° refocusing pulses, diminish magnetic susceptibility artifacts, thereby increasing the conspicuity of normal and abnormal structures in the internal auditory canal (10). Fast spin-echo images also retain true spin-echo T2 contrast features rather than the $T2^*$ contrast characteristics of gradient-echo techniques.

Fast spin-echo techniques allow multiple lines of k-space to be filled during a single TR, thereby significantly reducing acquisition time. This time savings can be used to obtain conventional spin echo–quality images faster or to obtain high-resolution images in an acquisition time comparable to that of a conventional spin-echo sequence. In our study, we attempted to maximize resolution while minimizing acquisition time by optimizing MR pulse sequence parameters. In pursuit of a high signal-to-noise ratio, we used a dual temporomandibular joint surface receiver coil system while transmitting with the body coil. Small surface coils provide inherently higher signal-to-noise ratios than standard head coils (12). Additionally, with a small field of view (17 cm), there is little wrap-around artifact, since the temporomandibular joint surface coils generate little signal outside this field of view.

In developing our protocol, we considered the four major components affecting scan time: scan time = TR × number of phase-encoding steps × number of excitations/echo train length. The longest echo train permissible at the time of the study, 16, was used in order to minimize scan time. Two major adverse consequences of increasing echo train length are the emergence of blurring artifacts, especially in the periphery of the image, and the reduction in the number of sections available if TR remains constant. Each line in k-space is acquired at a different echo delay, which means that the tissue has a different amount of transverse magnetization due to T2 decay. Filling the k-space data matrix in this manner commonly results in structured noise along the phase-encoding direction, with decreased signal-to-noise ratio compared with similar conventional spin-echo images produced with comparable scanning parameters (8). This blurring decreases as the number of phase-encoding steps is increased, and it is practically unnoticeable at 512 phase-encoding steps (14).

A rectangular matrix of 512 × 384 was chosen; the 384 phase-encoding steps used in our protocol represented a compromise between imaging time and blurring effects related to echo train length. The number of sections allowed is generally determined by the amount of sequence time taken up by each echo train. As the echo train lengthens, the amount of time required to generate a section during the MR experiment increases; consequently, TRs must be concomitantly lengthened to prevent a section penalty. Long TRs (4000 to 5000) were used to increase the number of sections available as well as to enhance T2 weighting and to increase the signal-to-noise ratio. The time savings related to echo train length also allowed four excitations to be used, resulting in an in-

crease in the signal-to-noise ratio (which is proportional to the square root of the number of excitations).

Fat saturation was used to remove high-signal-intensity fat found in the inner ear region on fast spin-echo sequences, which may be misinterpreted as an abnormal finding. The addition of a fat saturation radio frequency lobe to the MR experiment results in a slight section penalty; however, in a small area of interest, such as the internal auditory canal, the maximum number of sections that can be acquired with a fat-saturated fast spin-echo technique is more than adequate. Our fast spin-echo imaging protocol yields nine images of exquisite detail in an acquisition time of 8 minutes.

Having devised our version of the best alternative fast spin-echo limited MR examination available at the time, we then compared the standard of reference (enhanced T1-weighted conventional spin-echo images) for imaging the internal auditory canal/cerebellopontine angle with the high-resolution T2-weighted fast spin-echo images in a blinded fashion. As the results indicate, the alternative T2-weighted fast spin-echo images were nearly equivalent to the enhanced T1-weighted images in the diagnosis of acoustic schwannoma. The two false-negative results in the fast spin-echo group involved evaluation of the smallest tumors in our study group, $1 \times 1 \times 2$-mm (Fig 1) and $2 \times 2 \times 3$-mm schwannomas. Both small lesions were located within small internal auditory canals. Two false-positive results were also encountered, one each in the conventional spin-echo and fast spin-echo groups. Petrous apical fat was mistaken for an enhancing internal auditory canal mass on a single conventional spin-echo sequence. Nerve clumping in a small internal auditory canal was mistaken for a small acoustic schwannoma by one observer on the two-dimensional fast spin-echo images. Given the number of observations made in this study, these errors were not statistically significant. Small internal auditory canals were also present in these false-positive examinations.

On the fast spin-echo images, small internal auditory canals decreased the amount of high-intensity cerebrospinal fluid surrounding normal and abnormal seventh and eighth cranial nerves. Consequently, the observers were less confident in the evaluation of these images and were more likely to misinterpret the findings. At the time of this study, fast spin-echo imaging could be done only with 3-mm contiguous images. The continued rapid development of MR pulse sequences now allows most magnets to obtain 3-D fast spin-echo sequences with contiguous section thickness of 0.8 mm. We think that the three additional looks at the internal auditory canal for each of the sections we were able to review, made possible by this new technology, makes the prospect of missing a mass lesion of the internal auditory canal/cerebellopontine angle area even more unlikely.

A cost analysis of this process is difficult because of the large differences in the billed charges and the collected revenues in MR imaging today. However, concentrating on billed global charges alone, the average cost of a complete consultation by a head and neck surgeon in our institution to determine whether MR imaging should be ordered is as follows: physician visit = $150, complete audiometry = $70, impedance testing = $25, and brain stem evoked response = $250, for a total of $495. For a complete conventional spin-echo MR examination (sagittal T1 localizer, T2 fast spin-echo dual-echo whole-brain, axial and coronal internal auditory canal/cerebellopontine angle conventional spin-echo T1-weighted contrast-enhanced study), the total technical and professional cost is $1200. However, for the limited T2-weighted fast spin-echo examination (60-second coronal single-echo fast spin-echo localizer; axial and coronal high-resolution T2-weighted fast spin-echo study of the internal auditory canal/cerebellopontine angle), the total technical and professional charges are $400. This minimal charge is possible because of the less than 20 minutes of scanning time and the absence of contrast material. Since the initial study, we have moved to the use of the 60-second localizer and a single axial 3-D fast spin-echo sequence as our limited internal auditory canal/cerebellopontine angle study, with total scan times now under 10 minutes.

An overall assessment of the change in physician behavior and incurred expense that results reveals that the head and neck surgeons in our institution are no longer using impedance testing or brain stem evoked response in their work-up of unilateral sensorineural hearing loss. Instead, complete audiometric testing is done, and the limited MR examination is ordered directly if the audiogram suggests the possibility of acoustic schwannoma (asymmetric pure tone test and a disproportionate speech dis-

crimination score on the affected side). This direct referral saves $345 in tests, moving the patient immediately to the limited MR examination. The use of the limited MR examination saves $800 as compared with the global charge of the full MR examination. Finally, in the past, patients were often seen again in 6-month intervals by the head and neck surgeon to follow the evolution of equivocal unilateral sensorineural hearing loss with audiometric, impedance, and brain stem evoked response testing ($495 per visit). Excluding acoustic schwannoma at the outset of this process moves the patient back to the primary care provider after the initial visit when the MR findings are negative.

What about the other lesions along the central acoustic pathway that have been found to cause sensorineural hearing loss? The 60-second coronal localizer done with a larger field of view provides a limited look at the intraaxial components of the central acoustic pathway away from the immediate brain stem area. The high-resolution fast spin-echo limited study provides an excellent look at the subjacent pons and medulla area. It will also identify the other space-occupying masses of the internal auditory canal/cerebellopontine angle as filling defects, just as it does the acoustic schwannoma. However, the more subtle meningeal disorders and inflammatory intralabyrinthine lesions would be missed (15). At this point, the philosophy of a limited examination comes into play. As radiologists, we screen the body constantly with less expensive, less powerful imaging tools, accepting the obligate misses that come with this approach. For example, coronal sinus CT for sinusitis does not show brain lesions that might be causing headache. As the symptoms rise in severity, more costly examinations are used in the diagnostic scheme. In the case of limited MR imaging of the internal auditory canal/cerebellopontine angle, there will be infrequent instances in which the patient will return for a complete enhanced MR examination of the brain and the internal auditory canal/cerebellopontine angle.

Limited, unenhanced fast spin-echo MR imaging of the internal auditory canal/cerebellopontine angle provides inexpensive, high-resolution images of this anatomic area. After analyzing data generated from the study of patients with pathologically documented acoustic schwannoma and of control subjects, we have concluded that there is no statistically significant difference between enhanced T1-weighted conventional spin-echo and unenhanced high-resolution fast spin-echo MR techniques in the detection of acoustic schwannoma. Limited unenhanced high-resolution fast spin-echo MR imaging of the internal auditory canal/cerebellopontine angle is a cost-effective method for accurately diagnosing acoustic schwannoma and may become an alternative to the conventional enhanced MR techniques currently in use.

References

1. Slooff JL. Pathological anatomical findings in the cerebellopontine angle. *Adv Otorhinolaryngol* 1984;34:89
2. Kumar A, Maudelonde C, Mafee M. Unilateral sensory hearing loss: analysis of 200 consecutive cases. *Laryngoscope* 1986;96: 14–32
3. Armington WG, Harnsberger HR, Smoker WRK, Osborn AG. Normal and diseased acoustic pathway: evaluation with MR imaging. *Radiology* 1988;167:509–515
4. Gentry LR, Jacoby CG, Turski PA, Houston LW, Strother CM, Sackett JF. Cerebellopontine angle-petromastoid mass lesions: comparative study of diagnosis with MR imaging and CT. *Radiology* 1987;162:513–520
5. Enzmann DR, O'Donohue J. Optimizing MR imaging for detecting small tumors in the cerebellopontine angle and internal auditory canal. *AJNR Am J Neuroradiol* 1987;8:99–106
6. Schmalbrock P, Brogan MA, Chakeres DW, Hacker VA, Ying K, Clymer BD. Optimization of submillimeter resolution MR imaging methods for the inner ear. *J Magn Reson Imaging* 1993;451–459
7. Casselman JW, Kuhweide R, Deimling M, Ampe W, Dehaene I, Meeus L. Constructive interference in steady state: 3DFT MR imaging of the inner ear and cerebellopontine angle. *AJNR Am J Neuroradiol* 1993;14:47–57
8. Jones KM, Mulkern RV, Schwartz RB, Oshio K, Barnes PD, Jolesz FA. Fast spin-echo MR imaging of the brain and spine: current concepts. *AJR Am J Roentgenol* 1992;158:1313–1320
9. Kraemer HC. *Evaluating Medical Tests.* Newbury Park, Calif: Sage Publications; 1992:15
10. Tien RD, Felsberg GJ, Macfall J. Fast spin-echo high-resolution MR imaging of the inner ear. *AJR Am J Roentgenol* 1992;159: 395–398
11. Elster AD. Sellar susceptibility artifacts: theory and implications. *AJNR Am J Neuroradiol* 1993;14:129–136
12. Koenig H, Lenz M, Sauter R. Temporal bone region: high-resolution MR imaging using surface coils. *Radiology* 1986;159:191–194
13. Brogan M, Chakeres DW, Schmalbrock P. High-resolution 3DFT MR imaging of the endolymphatic duct and soft tissues of the otic capsule. *AJNR Am J Neuroradiol* 1991;12:1–11
14. Prorok RT, Sawyer AM. *Fast Imaging Techniques: Signa Advantage Applications Guide.* Milwaukee, Wis: General Electric Co; 1992;4:30–37
15. Mark AS, Seltzer S, Harnsberger HR. Sensorineural hearing loss: more than meets the eye? *AJNR Am J Neuroradiol* 1993;14: 37–45

Please see the Commentary on page 1226 in this issue.